Article

Cite This: Biomacromolecules 2019, 20, 1325−1333

pubs.acs.org/Biomac

Synthesis and Self-Assembly of Double-Hydrophilic and Amphiphilic Block Glycopolymers

Azis Adharis,[†] Thomas Ketelaar,[†] Amalina G. Komarudin,[‡] and Katja Loos*[,†]

[†]Macromolecular Chemistry and New Polymeric Materials, Zernike Institute for Advanced Materials, University of Groningen, Nijenborgh 4, 9747 AG Groningen, The Netherlands

[‡]Molecular Microbiology, Groningen Biomolecular Sciences and Biotechnology Institute, University of Groningen, Nijenborgh 7, 9747 AG Groningen, The Netherlands

Supporting Information

ABSTRACT: In this report, we present double-hydrophilic block glycopolymers of poly(2-hydroxyethyl methacrylate)-*b*-poly(2-(*β*-glucosyloxy)ethyl methacrylate) (PHEMA-*b*-PGEMA) and amphiphilic block glycopolymers of poly(ethyl methacrylate)-*b*-PGEMA (PEMA-*b*-PGEMA) synthesized via reversible addition−fragmentation chain transfer (RAFT) polymerization. The block glycopolymers were prepared in two compositions of P(H)EMA macro-chain transfer agents (CTAs) and similar molecular weights of PGEMA. Structural analysis of the resulting polymers as well as the conversion of (H)EMA and GEMA monomers were determined by ^{1}H NMR spectroscopy. Size exclusion chromatography measurements confirmed both P(H)EMA macro-CTAs and block glycopolymers had a low dispersity ($Đ \leq 1.5$). The synthesized block glycopolymers had a degree of polymerization and a molecular weight up to 222 and 45.3 kg mol^{-1}, respectively. Both block glycopolymers self-assembled into micellar structures in aqueous solutions as characterized by fluorescence spectroscopy, ultraviolet−visible spectroscopy, and dynamic light scattering experiments.

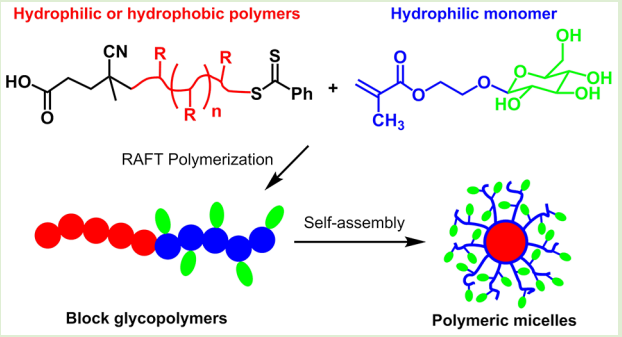

INTRODUCTION

Glycopolymers are synthetic polymers having sugar groups serving as pendant moieties.[1] Glycopolymers have received much attention due to their capability to mimic the biological function of glycolipids and glycoproteins, two macromolecules that are responsible for many cellular activities in the cell surface.[2] The sugar part of these macromolecules plays important roles, for instance during cell recognition and cell−cell adhesion to interact with sugar-binding proteins. Besides, this interaction is also involved in the processes of pathogen infection.[3] Therefore, researchers utilized glycopolymers notably as models to study subjects related to human health including inhibitors of diseases,[4−6] drug delivery materials,[7−9] biosensors,[10,11] and immunotherapy.[12−14]

Glycopolymers have been prepared in different kinds of architectures such as linear homopolymers, dendrimers, star polymers, random and block copolymers.[15−19] The block copolymers of glycopolymer, later called as block glycopolymers, have gained much interest especially due to their ability to create spherical particles in solution via self-assembly processes forming various morphologies like micelles, vesicles, and particles at nanometer scales.[20−22] Two types of block glycopolymers were identified namely amphiphilic block glycopolymer (ABG) and double-hydrophilic block glycopolymer (DHBG). Most studies were focused on ABG which resemble commonly available low molecular weight surfactants in terms of their structure. The ABGs consist of a hydrophilic part of sugar-based polymers and a hydrophobic group of polymers or small molecules.

Having learned from nature where many hydrophilic polymers possess a pivotal function in biological processes, the literature on the synthesis of DHBGs has grown recently.[23−28] In addition, preparation of DHBGs can often be easily performed in aqueous media rather than using organic solvents that are usually needed for the synthesis of ABGs. As a result, this can avoid the necessary protection/deprotection steps of the hydroxyl groups of sugars during the polymer synthesis. Many reports on DHBGs involved a hydrophilic sugar-based polymer and another block of a hydrophilic thermoresponsive polymer that, regrettably, transformed into hydrophobic polymer upon stimulation.[25−28] For example, hydrophilic poly(di(ethylene glycol)methyl ether methacrylate) and poly(*N*-isopropylacrylamide) which possess a lower critical solution temperature were commonly used in this system. Consequently, the synthesized DHBGs turned into

Received: November 30, 2018
Revised: January 14, 2019
Published: January 17, 2019

DOI: 10.1021/acs.biomac.8b01713
Biomacromolecules 2019, 20, 1325−1333

ABGs after the thermal stimulation was implemented in order for the block copolymers to be self-assembled.

In this study, we report the synthesis of DHBGs that are able to self-assemble without any external trigger. The block glycopolymers are composed of hydrophilic poly(2-hydroxyethyl methacrylate) (PHEMA) and poly(2-(β-glucosyloxy)-ethyl methacrylate) (PGEMA). PHEMA was regarded as a biocompatible polymer whereas the monomer of PGEMA was enzymatically synthesized from biobased resources. Hence, the synthesized DHBGs of PHEMA-*b*-PGEMA may be suited for biorelated application materials. Preparation of the DHBGs was carried out by reversible addition−fragmentation chain transfer (RAFT) polymerization in DMF, yet protection/deprotection steps of the hydroxyl group of monomer GEMA were not necessary. Park et al. reported similar DHBGs, that consisted of PHEMA and poly(2-*O*-(*N*-acetyl-β-D-glucosamine)ethyl methacrylate), synthesized via atom transfer radical polymerization.[24] Unfortunately, this method leaves traces of metal catalyst in the final product hindering the polymer to be used for biomedical purposes. Moreover, we also synthesized ABGs by replacing PHEMA with hydrophobic poly(ethyl methacrylate) (PEMA). The spontaneous self-assembly of the prepared DHBGs and ABGs was successfully characterized by fluorescence spectroscopy, UV−vis spectroscopy, and dynamic light scattering experiments.

EXPERIMENTAL SECTION

Materials. 4-Cyano-4-(phenylcarbonothioylthio)pentanoic acid (CPADB) >97% was obtained from Sigma-Aldrich. *N*,*N*-Dimethylformamide (DMF) 99+% extra pure was purchased from Acros Organics. Ethanol (EtOH), pentane, chloroform ($CHCl_3$), and diethyl ether were acquired from Avantor. All chemicals were used as received. α,α′-Azoisobutyronitrile (AIBN) >98% was obtained from Sigma-Aldrich and recrystallized twice from methanol prior to use. 2-Hydroxyethyl methacrylate (HEMA) 98% and ethyl methacrylate (EMA) 99% were purchased from Sigma-Aldrich, and purification was done by passing them through the basic Al_2O_3 column. 2-(β-glucosyloxy)ethyl methacrylate (GEMA) monomer was synthesized according to literature.[29]

Methods. *^{1}H Nuclear Magnetic Resonance (NMR) Spectroscopy.* ^{1}H NMR spectra were recorded on a 400 MHz Varian VXR Spectrometer with DMSO-d_6 (99.5 atom % D, Aldrich) used as the solvent. The attained spectra were analyzed by MestReNova Software from Mestrelab Research S.L.

Size Exclusion Chromatography (SEC). SEC was done on a Viscotek GPCmax equipped with model 302 TDA detectors and the eluent of DMF containing 0.01 M LiBr at a flow rate of 1.0 mL min^{-1}. Three columns were used: a guard column (PSS-GRAM, 10 μm, 5 cm) and two analytical columns (PSS-GRAM-1000/30 Å, 10 μm, 30 cm). The temperature for the columns and detectors were at 50 °C. The samples (PHEMA, PEMA, PHEMA-*b*-PGEMA, PEMA-*b*-PGEMA) were filtered through a 0.45 μm PTFE filter prior to injection. Narrow PMMA standards were utilized for calibration and molecular weights were calculated by the universal calibration method using the refractive index increment of PMMA (0.063 mL g^{-1}).

For PEMA samples, SEC measurements were also performed on a Viscotek GPC equipped with three detectors (Viscotek Ralls detector, Viskotek Viscometer Model H502, and Schambeck RI2012 refractive index detector), a guard column (PLgel 5 μm Guard, 50 mm), and two analytical columns (PLgel 5 μm MIXED-C, 300 mm, Agilent Technologies) at 35 °C. THF 99+% (stabilized with BHT) was applied as the eluent at a flow rate of 1.0 mL min^{-1}. Narrow polystyrene standards were utilized for calibration and molecular weights were calculated by the universal calibration method using the refractive index increment of PEMA (0.085 mL g^{-1}, obtained from Polymer Source Inc.). Data acquisition and calculations were performed by Viscotek OmniSec software version 5.0 for both SEC experiments.

Fluorescence Spectroscopy. The fluorescence emission spectra were measured with a QuantaMaster 40 Spectrofluorimeter (Photon Technology International) using pyrene molecules as the fluorescence probe. Various concentrations of diblock glycopolymers ranging from 0.05 to 5 mg mL^{-1} were mixed with pyrene (2 μM) and the samples were incubated overnight in the dark at room temperature. Pure Milli-Q water and Milli-Q water containing DMF (up to 2.5 mmol %) were utilized as the solvent for PHEMA-*b*-PGEMA and PEMA-*b*-PGEMA samples, respectively. Measurements were carried out by exciting the pyrene at 334 nm and the emission spectra were scanned from 350 to 470 nm with excitation and emission slits of 8 and 2 nm. Critical micelle concentrations (CMC) of the samples were determined from the inflection point of the plot between the fluorescence intensity ratios of pyrene at 373 nm (I_1) and 383 nm (I_3) against the concentration logarithm of the samples.

UV−Visible Spectroscopy. The absorption spectra were measured with a Spectramax M3 spectrophotometer (Molecular Devices) using benzoylacetone molecules as the absorption probe. Various concentrations of diblock glycopolymers ranging from 0.05 to 5 mg mL^{-1} were mixed with benzoylacetone (0.7 μM) and the samples were incubated overnight in the dark at room temperature. Pure Milli-Q water and Milli-Q water containing DMF (up to 2.5 mmol %) were utilized as the solvent for PHEMA-*b*-PGEMA and PEMA-*b*-PGEMA samples, respectively. The samples were put on a quartz cuvette QS 104 (Hellma Analytics) and the absorption spectra were recorded from 200 to 400 nm.

Dynamic Light Scattering (DLS). DLS measurements were done on an ALV/CGS-3 Compact Goniometer System equipped with HeNe laser (JDS Uniphase, model 1218−2, 632.8 nm, 22 mW) and an ALV/LSE-5004 multiple tau digital correlators. All measurements were carried out in triplicate at room temperature, at scattering angles between 30° and 150° with a 10° interval and toluene (Chromasolv Plus) was utilized as the immersion liquid. Pure Milli-Q water and Milli-Q water containing DMF (up to 2.5 mmol %) were utilized as the solvent for PHEMA-*b*-PGEMA and PEMA-*b*-PGEMA samples, respectively. The concentration of sample solution was 5 mg mL^{-1}, thus above the CMC. The solvent and the samples were filtered at least 3 times through cellulose acetate filters (0.20 μm for the solvent and 0.45 μm for the samples) prior to measurement. The measured autocorrelation functions were transformed to distribution functions by regularized fit setup (g2(t)) of the ALV-Correlator software (version 3.0). The translational diffusion coefficient (D_t) is obtained from the plot of the decay rates (Γ, equal to the decay time^{-1}(τ^{-1})) of the distribution functions against the square of the scattering vectors (q) following eq 1. Hydrodynamic diameter (D_h in nm) of the micelles was calculated by Stokes−Einstein relation (see eq 2) where K_b, T, and η are the Boltzmann constant (J K^{-1}), temperature (K), and the viscosity (mPa s), respectively. The viscosity was obtained following the reference.[30]

$$\frac{1}{\tau} = \Gamma = D_t \cdot q^2 \tag{1}$$

$$D_h = \frac{K_b \cdot T}{3\pi \cdot \eta \cdot D_t} \tag{2}$$

Synthesis of P(H)EMA Macro-CTAs by RAFT Polymerization. The synthesis of P(H)EMA macro-CTAs was performed according to literature with some modifications.[31] In a 25 mL round-bottom flask was dissolved HEMA (3.50 g, 3.262 mL, 26.89 mmol) or EMA (3.50 g, 3.815 mL, 30.66 mmol) in EtOH. A calculated amount of CPADB (RAFT agent) from a stock solution was injected into the monomer solution while stirring and the flask was sealed with a rubber septum, put in an ice bath, and purged by N_2 for at least 1 h. The reaction was started by adding a calculated amount of AIBN from a stock solution into the reaction mixture and puting the flask in an oil bath at 70 °C. After 7 h, an aliquot solution (100 μL) was drawn for determination of the monomer conversion by ^{1}H NMR and the flask was then put in an ice bath to stop the reaction. The polymer was isolated by

DOI: 10.1021/acs.biomac.8b01713
Biomacromolecules 2019, 20, 1325−1333

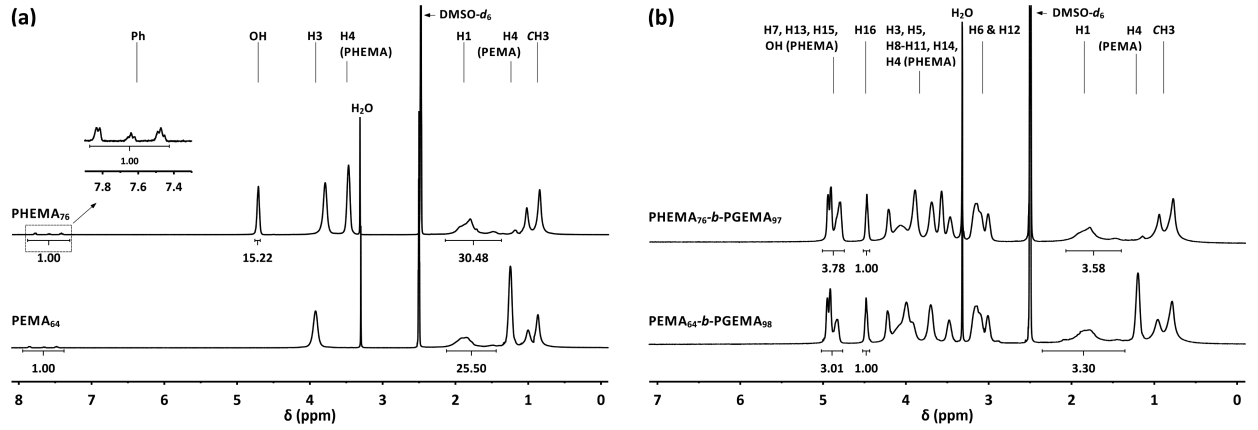

Figure 1. ^{1}H NMR spectra of (a) PHEMA$_{76}$ and PEMA$_{64}$ macro-CTAs as well as (b) PHEMA$_{76}$-*b*-PGEMA$_{97}$ and PEMA$_{64}$-*b*-PGEMA$_{98}$.

precipitation into a cold solvent (10x volume) and reprecipitated at least two times. $CHCl_3$ and pentane were used as the solvent for PHEMA and PEMA, respectively. The obtained polymers were dried in a vacuum oven (40 °C) overnight. The polymers were synthesized in two compositions with a ratio [(H)EMA]:[CPADB]:[AIBN] of 100:1:0.2 and 200:1:0.2.

Calculation of the (H)EMA conversion was performed following eq 3 where I_{H1} is the peak integration of the proton (H1) of the polymer backbone and $I_{monomer}$ is the peak integration of the vinyl proton of the unreacted monomer in the reaction mixture (^{1}H NMR spectra are shown in Figure S1a). The theoretical molecular weight ($M_{n,theory}$) of the synthesized P(H)EMA was calculated by eq 4. The degree of polymerization (DP_n) of P(H)EMA was determined by eq 5 where I_{Ph} is the peak integration of the phenyl proton (Ph) of the RAFT agent (see Figure 1a). Calculation of the molecular weight ($M_{n,NMR}$) of the synthesized P(H)EMA was performed by eq 6.

$$\text{conv. (\%)} = \frac{I_{H(polymer)}}{I_{H(monomer)} + I_{H(polymer)}} \times 100\% = \frac{I_{H1}/2}{I_{monomer} + (I_{H1}/2)} \times 100\% \quad (3)$$

$$M_{n,theory} = \left(\frac{[monomer]}{[RAFT\ agent]} \times \text{conv.} \times MW_{monomer}\right) + MW_{RAFT\ agent} \quad (4)$$

$$DP_n = \frac{I_{H(polymer)}}{I_{H(end\text{-}group)}} = \frac{I_{H1}/2}{I_{Ph}/5} \quad (5)$$

$$M_{n,NMR} = (DP_n \times MW_{monomer}) + MW_{RAFT\ agent} \quad (6)$$

PHEMA. Pinkish powder, monomer conversion: 57% (PHEMA$_{76}$) and 51% (PHEMA$_{125}$), yield: 49% (PHEMA$_{76}$) and 34% (PHEMA$_{125}$). ^{1}H NMR (DMSO-d_6, 400 MHz) δ in ppm: 7.35−7.93 (m, Ph), 4.75 (s, *OH*), 3.82 (s, H3), 3.50 (s, H4), 1.39−2.16 (br, H1), 0.62−1.26 (br, *CH*$_3$-polymer backbone).

PEMA. Pinkish powder, monomer conversion: 56% (PEMA$_{64}$) and 50% (PEMA$_{107}$), yield: 35% (PEMA$_{64}$) and 25% (PEMA$_{107}$). ^{1}H NMR (DMSO-d_6, 400 MHz) δ in ppm: 7.37−7.95 (m, Ph), 3.92 (s, H3), 1.44−2.12 (br, H1), 1.24 (s, H4), 0.7−1.11 (m, *CH*$_3$-polymer backbone).

Synthesis of P(H)EMA-*b*-PGEMA Diblock Glycopolymers by RAFT Polymerization. In a 10 mL round-bottom flask was prepared 1.2 M monomer solution by dissolving GEMA (0.56 g, 1.91 mmol) in DMF. 1 mol % of the P(H)EMA macro-CTA was added into the monomer solution while stirring and the flask was sealed with a rubber septum, put in an ice bath, and purged by N_2 for at least 1 h. The reaction was started by adding a calculated amount of AIBN from a stock solution into the reaction mixture and put the flask in an oil bath at 65 °C. The ratio of [GEMA]:[P(H)EMA]:[AIBN] was 100:1:0.2. After 18 h, an aliquot solution (100 μL) was drawn for determination of the GEMA conversion by ^{1}H NMR and the flask was then put in an ice bath to stop the reaction. The polymer was isolated by precipitation into a cold solvent (10× volume) and reprecipitated two times. THF and a mixture of diethyl ether/pentane (1/1) were used for PHEMA-*b*-PGEMA and PEMA-*b*-PGEMA, respectively. The obtained polymers were dried in a vacuum oven (40 °C) overnight.

Calculation of the GEMA conversion was performed following eq 7 where I_{H7} is the peak integration of all anomeric protons (H7) of the glucose, derived from the unreacted monomer and the side-chain of the polymer, in the reaction mixture. ^{1}H NMR spectra of the reaction mixture are available in Figure S1b. $M_{n,theory}$ of PGEMA block was calculated by eq 4. DP_n of PGEMA block was determined by comparing the composition of PGEMA with P(H)EMA using the integral region of their respective protons obtained from the ^{1}H spectra as displayed in Figure 1b (see eq 8). $M_{n,NMR}$ of PGEMA was calculated by eq 6 and molecular weight of the prepared diblock glycopolymers was obtained by combining $M_{n,NMR}$ of both P(H)EMA and PGEMA blocks.

$$\text{conv. (\%)} = \frac{I_{H7} - I_{monomer}}{I_{H7}} \times 100\% \quad (7)$$

$$DP_{n,PGEMA} = \frac{I_{H(PGEMA)}}{I_{H(P(H)EMA)}} \times DP_{n,P(H)EMA} = \frac{I_{H7}}{(I_{H1}/2) - I_{H7}} \times DP_{n,P(H)EMA} \quad (8)$$

PHEMA-b-PGEMA. Pale pinkish powder, GEMA conversion: 98% (PHEMA$_{76}$-*b*-PGEMA$_{97}$) and 99% (PHEMA$_{125}$-*b*-PGEMA$_{97}$), yield: 70% (PHEMA$_{76}$-*b*-PGEMA$_{97}$) and 73% (PHEMA$_{125}$-*b*-PGEMA$_{97}$). ^{1}H NMR (DMSO-d_6, 400 MHz) δ in ppm: 4.93 (d, J = 12 Hz, H7), 4.75−5.02 (m, H7, H13, H15, *OH*), 4.48 (s, H16), 3.39−4.32 (m, H3, H4, H5, H8−H11, H14), 2.93−3.25 (m, H6, H12), 1.39−2.07 (br, H1), 0.62−1.22 (m, *CH*$_3$-polymer backbone).

PEMA-b-PGEMA. Pale pinkish powder, GEMA conversion: 99% (PEMA$_{64}$-*b*-PGEMA$_{98}$) and 99% (PEMA$_{107}$-*b*-PGEMA$_{98}$), yield: 77% (PEMA$_{64}$-*b*-PGEMA$_{98}$) and 68% (PEMA$_{107}$-*b*-PGEMA$_{98}$). ^{1}H NMR (DMSO-d_6, 400 MHz) δ in ppm: 4.93 (d, J = 13.6 Hz, H7), 4.76−5.02 (m, H7, H13, H15), 4.48 (s, H16), 3.39−4.32 (m, H3, H5, H8−H11, H14), 2.93−3.25 (m, H6, H12), 1.35−2.35 (br, H1), 1.2 (s, H4), 0.62−1.30 (m, *CH*$_3$-polymer backbone).

RESULTS AND DISCUSSION

Synthesis of Macro-CTAs. RAFT polymerization is one of the controlled polymerization techniques that has been widely utilized to prepare well-defined structures of homopolymers and block copolymers.[32−34] In general, this technique is able to

DOI: 10.1021/acs.biomac.8b01713
Biomacromolecules 2019, 20, 1325−1333

Scheme 1. Synthesis of (a) PHEMA (R = OH) and PEMA (R = H) Macro-CTAs as well as (b) P(H)EMA-*b*-PGEMA Using RAFT Polymerization

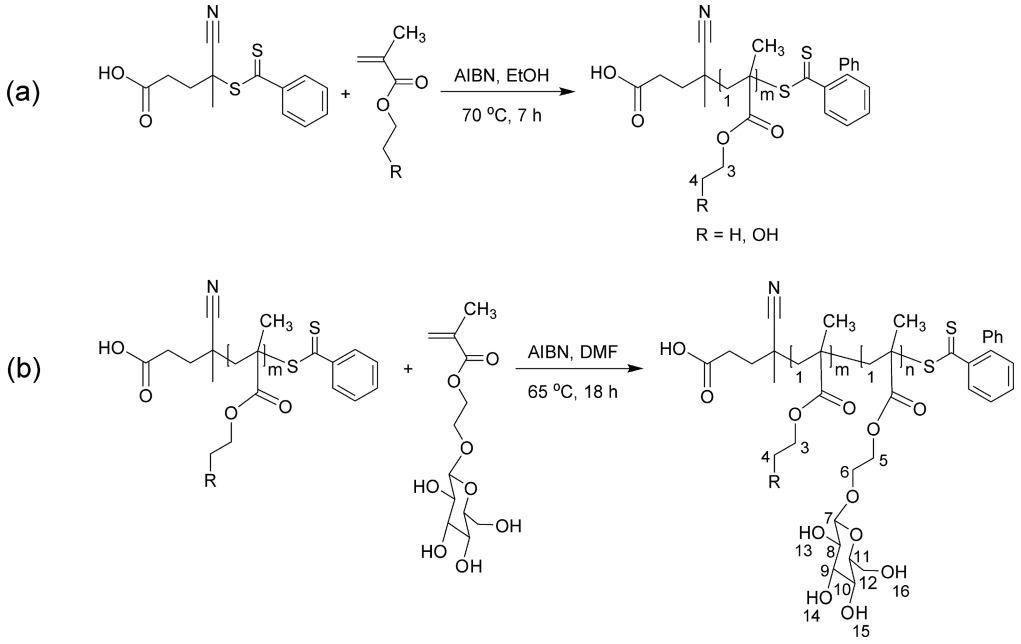

Table 1. Overview of the Synthesized P(H)EMA Macro-CTAs

macro-CTAs	[monomer][a]	[RAFT agent][b]	[AIBN][b]	conv. (%)	$M_{n,theory}$[c]	$M_{n,NMR}$[c]	$M_{n,SEC}$[c]	$Đ$
$PHEMA_{76}$	2.7	27.0	5.4	58	8.1	10.2	22.5	1.12
$PHEMA_{125}$	2.7	13.5	2.7	54	14.7	16.6	32.6	1.20
$PEMA_{64}$	2.7	27.0	5.4	58	6.9	7.6	2.5	1.30
$PEMA_{107}$	2.7	13.5	2.7	53	12.4	12.4	5.7	1.21

[a][Monomer] in M. [b][RAFT agent] and [AIBN] in mM. [c]Molecular weights in kg mol^{-1}.

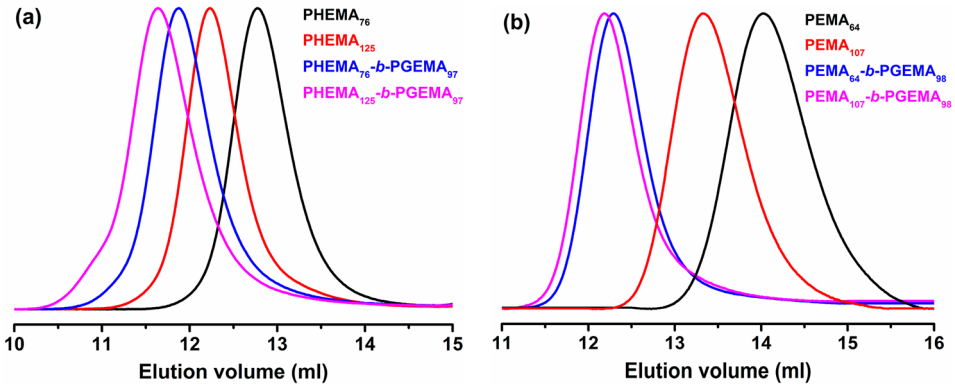

Figure 2. SEC measurements (RI signals) of the synthesized (a) PHEMA macro-CTAs and PHEMA-*b*-PGEMA as well as (b) PEMA macro-CTAs and PEMA-*b*-PGEMA.

polymerize a large range of monomers in numerous reaction media using an initiator in combination with a chain transfer agent (CTA). Since the CTA plays a crucial part to control the length of the polymer chain, this molecule must be carefully selected. 4-Cyano-4-(phenylcarbonothioylthio)pentanoic acid (CPADB) is a commercially available dithioester-based CTA that is commonly used for the polymerization of methacrylate and methacrylamide monomers. The resulted homopolymers synthesized by RAFT polymerization typically contain two functional groups at each end of the polymer chains which was derived from the CTA. These homopolymers are called macro-CTAs that can further react with other monomers to form block copolymers.

Scheme 1a shows the synthesis of P(H)EMA macro-CTAs with two different chain lengths employing AIBN as the thermal initiator in ethanolic solution. The monomer conversion was determined by eq 3 and was kept below 60% in order to minimize the loss of dithiobenzoyl end groups. The obtained conversion can be used to calculate the theoretical molecular weight ($M_{n,theory}$) following eq 4. The monomer conversion and molecular weights of the macro-CTAs are summarized in Table 1.

DOI: 10.1021/acs.biomac.8b01713
Biomacromolecules 2019, 20, 1325−1333

Table 2. Overview of the Synthesized P(H)EMA-*b*-GEMA

diblock glycopolymers[a]	conv. (%)	$M_{n,PGEMA}$[b]	$M_{n,PGEMA}$[c]	$M_{n,P(H)EMA\text{-}b\text{-}PGEMA}$[d]	$Đ$
$PHEMA_{76}$-*b*-$PGEMA_{97}$	98	29.0	28.7	38.9	1.37
$PHEMA_{125}$-*b*-$PGEMA_{97}$	99	29.3	28.7	45.3	1.51
$PEMA_{64}$-*b*-$PGEMA_{98}$	99	29.3	29.0	36.6	1.36
$PEMA_{107}$-*b*-$PGEMA_{98}$	99	29.3	29.0	41.4	1.34

[a][GEMA]:[P(H)EMA]:[AIBN] = 100:1:0.2. [b]$M_{n,theory}$ and [c]$M_{n,NMR}$ of PGEMA in kg mol^{-1}. [d]M_n of diblock glycopolymers by combining the $M_{n,NMR}$ of both block.

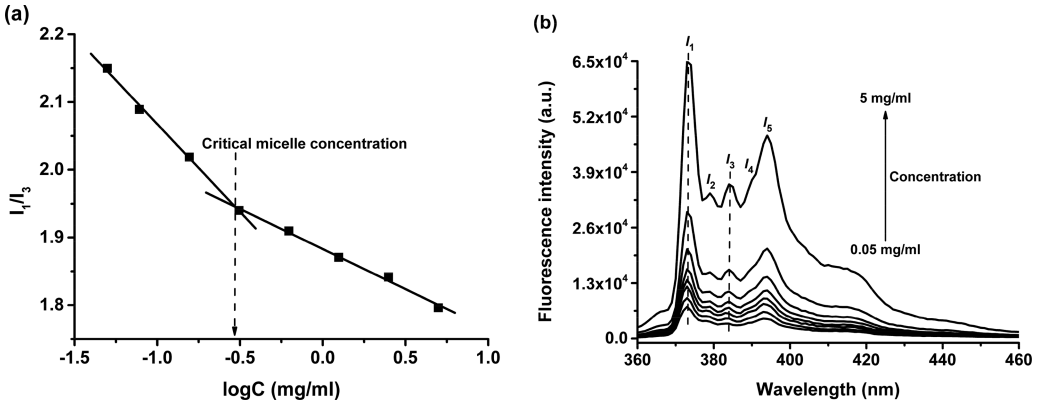

Figure 3. (a) Plot of the intensity ratio (I_1/I_3) of pyrene as the fluorescent probe vs the log concentrations of $PHEMA_{125}$-*b*-$PGEMA_{97}$. (b) Fluorescence emission spectra of pyrene at various $PHEMA_{125}$-*b*-$PGEMA_{97}$ concentrations.

The structure of P(H)EMA macro-CTAs was characterized by ^{1}H NMR spectroscopy as depicted in Figure 1a. Typical proton peaks of the polymer backbone were clearly observed around 0.5−2 ppm, while vinyl proton peaks of the monomer between 5.5 and 6 ppm disappeared, proving the successful polymerization. Other proton peaks (H3, H4, and OH) were clearly observable in the ^{1}H NMR spectra of the purified macro-CTAs. Besides, three proton signals belonging to the aromatic phenyl group around 7.5−8 ppm were detected that indicates the attachment of dithiobenzoyl group at the end of the polymer chain. Comparison of the peak integration of the proton at the polymer backbone and the proton at the end group (eq 5) results in a degree of polymerization (DP_n) of P(H)EMA macro-CTAs up to 125 with a maximum molecular weight ($M_{n,NMR}$) of 16.6 kg mol^{-1} according to eq 6.

SEC analysis of the P(H)EMA macro-CTAs are shown in Figure 2 with relatively narrow and monomodally distributed peaks of the retractive index signals. In combination with the low dispersity ($Đ$) as presented in Table 1, these results suggested that the macro-CTAs have been synthesized in a controlled way via RAFT polymerization. Furthermore, $M_{n,SEC}$ of PHEMA macro-CTAs were found to be overestimated while $M_{n,SEC}$ of PEMA macro-CTAs were underestimated in comparison with their respective $M_{n,\,theory}$ and $M_{n,NMR}$. The refractive index increment (dn/dc) of PMMA was used for the calculation and the differences in hydrodynamic volumes of standard PMMA and the synthesized P(H)EMA are responsible for the inaccuracy of the molecular weight determined by SEC measurement. This phenomenon was also reported in the literature.[31,35,36] When the correct dn/dc in an appropriate solvent was utilized for PEMA macro-CTAs (see Figure S2 and Table S1), similar numbers of $M_{n,SEC}$ as compared with $M_{n,theory}$ and $M_{n,NMR}$ were obtained.

Synthesis of DHBGs and ABGs. PHEMA and PGEMA are supposed to have hydrophilic properties due to the hydroxy groups available at the side chain of the polymer backbone that are able to form hydrogen bonds with water molecules. On the other hand, PEMA contains only nonpolar ethyl groups as the pendant moieties which makes the polymer more hydrophobic. Therefore, the combination of PHEMA or PEMA with PGEMA leads to the formation of double-hydrophilic block glycopolymers (DHBGs) or amphiphilic block glycopolymers (ABGs).

Preparation of P(H)EMA-*b*-PGEMA by RAFT polymerization was conducted according to the same principal with GEMA, AIBN, and DMF as the monomer, initiator, and solvent, respectively, as pointed out in Scheme 1b. However, CPADB, the chain transfer agent in the former reaction, was replaced by P(H)EMA macro-CTAs. The polymerization proceeded overnight with GEMA was almost fully converted according to eq 7. Using the latter result, we were able to determine the $M_{n,theory}$ of the PGEMA block by eq 4 (see Table 2).

Figure 1b represents the ^{1}H NMR spectra of P(H)EMA-*b*-PGEMA. In comparison with the ^{1}H NMR spectra of P(H)EMA macro-CTAs in Figure 1a, additional proton peaks between 3 and 5 ppm were observed that belong to the proton of the glucosyl unit of GEMA. For example, a doublet peak at 4.93 ppm corresponded to the typical anomeric proton of glucose in axial position. This finding indicates that the GEMA monomer was successfully reacted with P(H)EMA macro-CTAs forming block glycopolymers.

DP_n of the PGEMA block was determined by comparing the composition of PGEMA with P(H)EMA using the integral region of their respective protons from the ^{1}H spectra (See eq 8) and similar numbers of $M_{n,theory}$ and $M_{n,NMR}$ were obtained. Furthermore, SEC measurements of the synthesized P(H)-EMA-*b*-PGEMA are presented in Figure 2. The maxima of the refractive index signal of the block glycopolymers were shifted to a lower elution volume compared to P(H)EMA homopolymers proving that the chain extension of macro-CTAs by GEMA monomer was achieved. As a result, the block

DOI: 10.1021/acs.biomac.8b01713
Biomacromolecules 2019, 20, 1325−1333

glycopolymers have higher molecular weight than its P(H)EMA precursors. In addition, the macro-CTAs performed well on controlling the polymerization as shown by the elugrams of the block glycopolymers possessing relatively narrow peaks and an unimodal distribution. However, the dispersity of the block glycopolymers is a little bit higher than its precursor possibly because of the P(H)EMA macro-CTAs is less efficient as a chain transfer agent than CPADB molecules.

Self-Assembly of DHBGs and ABGs in Aqueous Solutions. PHEMA is defined as a hydrophilic polymer; however, its solubility in water is molecular weight dependent.[36] For instance, PHEMAs with molecular weights less than 3000 g mol^{-1} are fully soluble, between 3000 and 6000 g mol^{-1} they are only soluble at a certain temperature, and above 6000 g mol^{-1}, they are insoluble at any temperatures. In addition, this PGEMA is a completely water-soluble polymer. When two homopolymers have an opposite solubility in a solvent, their block copolymers are expected to aggregate by self-assembly processes in that particular solvent. In our case, the aggregation of these DHBGs was assumed to form spherical polymeric micelles with the PHEMA block serving as the core and the PGEMA block as the corona in aqueous solutions. A similar principle was also reported in the literature where block copolymers of water-insoluble yet hydrophilic polysaccharides and water-soluble polymers were phase separated into polymeric vesicles.[37−39] For a comparison purpose, we also prepared ABGs of hydrophobic PEMA and hydrophilic PGEMA.

Fluorescence spectroscopy is one of the well-established methods to characterize the formation of micelles, as well as to determine the critical micelle concentration (CMC) by using pyrene as a probe molecule.[40−42] The fluorescence emission spectra of pyrene are shown in Figure 3b with their typical five vibrational peaks clearly observable under different DHBG concentrations. At low concentrations of $PHEMA_{125}$-*b*-$PGEMA_{97}$, these peaks have a low intensity because the pyrene is mainly surrounded by water molecules. However, when the concentration of the samples increased, the fluorescence band also increased as a response to the less polar environment that was sensed by the pyrene. Under this circumstances, the pyrene molecules are entrapped in the interior of micelles. Additionally, the intensity ratio of the first and third vibrational peaks (I_1/I_3) was changed in line with the change of the sample concentrations. By plotting this ratio against the concentration logarithm of the sample (Figure 3a), the CMC of this DHBG micelle was determined to be at 0.30 mg mL^{-1} (7.25 μM). A similar number was obtained for $PHEMA_{76}$-*b*-$PGEMA_{97}$ and the ABGs (see Figure S3 and Table 3). These numbers are remarkably lower compared to the CMC of commonly available surfactants that range around 87 to 4 × 10^5 μM[43] and within the CMC range of some amphiphilic block copolymers micelles (0.1−3 × 10^3 μM).[44−46] It is evident that polymeric surfactants are more efficient in creating micelles than the low molecular weight ionic and nonionic surfactants.

Table 3. CMC and Hydrodynamic Diameter (D_h) of the Synthesized DHBGs and ABGs

diblock glycopolymers	CMC[a]	CMC[b]	D_h[c]
$PHEMA_{76}$-*b*-$PGEMA_{97}$	0.29	n/a	8.5
$PHEMA_{125}$-*b*-$PGEMA_{97}$	0.30	n/a	9.9
$PEMA_{64}$-*b*-$PGEMA_{98}$	0.25	0.31	15.1
$PEMA_{107}$-*b*-$PGEMA_{98}$	0.27	0.31	20.9

[a]Determined by fluorescence spectroscopy (in mg mL^{-1}). [b]Determined by UV−vis spectroscopy (in mg mL^{-1}). [c]Hydrodynamic diameter in nm. n/a = not applicable.

In order to gain more insight in the characteristic of the micelles core, UV−vis spectroscopy was performed with benzoylacetone (BZA) molecules serving as the absorption probe.[41,47] BZA are able to tautomerize in the ketonic and enolic form and the percentage of each form depends on the environment polarity. For example, the ketonic form will be dominant when BZA interacts with relatively polar surrounding via intermolecular hydrogen bonds of its carbonyl group. On the other hand, the enolic form will be more pronounced due to the formation of the intramolecular hydrogen bond in less polar or hydrophobic environment. Both ketonic and enolic forms can be detected at the absorption band of 250 and 312 nm, respectively.

Figure 4a exhibits the absorption spectra of BZA at different ABG concentrations of $PEMA_{107}$-*b*-$PGEMA_{98}$ and similar spectra were found for the $PEMA_{64}$-*b*-$PGEMA_{98}$. Below the concentration of 0.31 mg mL^{-1}, the peak intensity at 250 and 312 nm was constant. However, the intensity of the former peak decreased whereas the latter peak increased at the concentration above 0.31 mg mL^{-1}. Hence, the tautomeric equilibrium of BZA was shifted from the ketonic to the enolic form suggesting that most BZA was trapped inside the hydrophobic PEMA core of these ABG micelles. The concentration of 0.31 mg mL^{-1}, which was the starting point of changes in the BZA spectra, was defined as the CMC of this system. Nevertheless, there is no change of absorption spectra of BZA, i.e., the peak intensity at 250 nm remains higher than at 312 nm for DHBG samples as shown in Figure 4b. This is reasonable as the interior of these DHBG micelles consists of hydrophilic PHEMA in which the hydroxy groups of this polymer can stabilize the ketonic tautomer of BZA by means of intermolecular hydrogen bonding. Consequently, the CMC of the DHBG micelles could not be determined by this method.

DLS experiments were carried out to determine the hydrodynamic diameter of the self-assembled DHBG and ABG micelles in aqueous solutions. For this purpose, the samples were prepared at the concentration of 5 mg mL^{-1} which is clearly above the CMC. The measurements were performed at scattering angles between 30° and 150° with a 10° interval. The obtained autocorrelation functions were transformed into distribution functions and the results are displayed in Figure 5b. The dominant peaks at around 0.1−0.5 ms^{-1} corresponded to the micellar structures whereas the minor peaks between 2 and 6 ms^{-1} relate with the random-coil single chain structures of the block glycopolymers. The decay rate of the distribution function was fitted linearly against the q^2 (Figure 5a) and the slope of this plot was attributed to the translational diffusion coefficient parameter (D_t) in eq 1.[48,49] Using the gained D_t, hydrodynamic diameter of the micelles were calculated by the Stokes−Einstein Equation (eq 2), and the numbers are shown in Table 3.

The prepared DHBG and ABG micelles were different in chain lengths of P(H)EMA and the core properties (hydrophilic PHEMA vs hydrophobic PEMA). According to the DLS results, DHBG with a longer PHEMA block has a higher hydrodynamic diameter than its shorter counterpart at the same PGEMA block length. A similar pattern was also found in the ABG and these observations corresponded to the interior

DOI: 10.1021/acs.biomac.8b01713
Biomacromolecules 2019, 20, 1325−1333

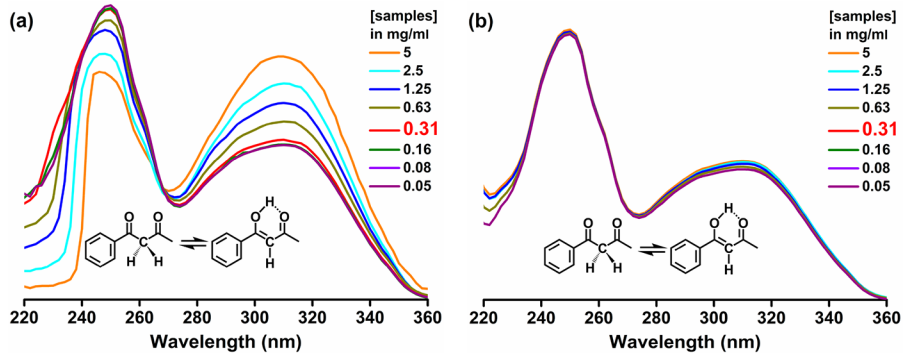

Figure 4. Absorption spectra of BZA in (a) ABGs and (b) DHBGs.

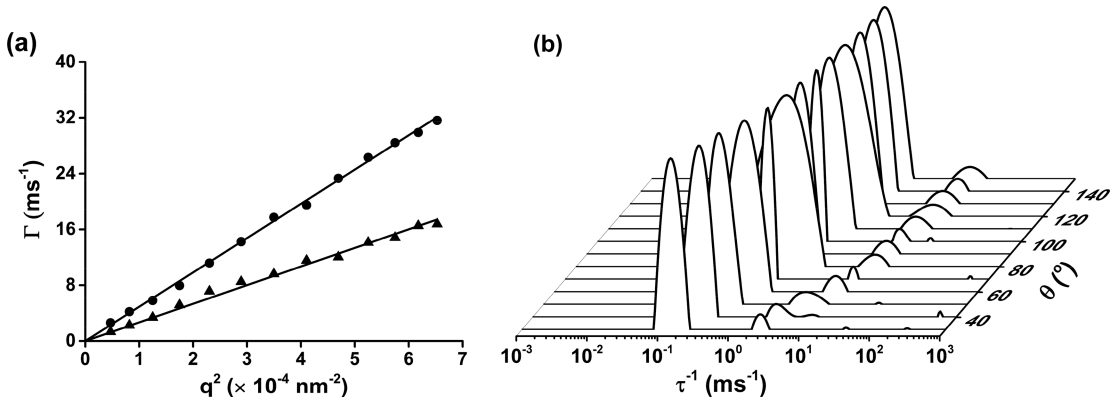

Figure 5. (a)Linear regression of the decay rate (Γ) with the square of scattering vectors (q^2) for the $PHEMA_{125}$-*b*-$PGEMA_{97}$ (●) and $PEMA_{64}$-*b*-$PGEMA_{98}$ (▲). (b) Normalized distribution functions of $PHEMA_{125}$-*b*-$PGEMA_{97}$ at different scattering angles.

size enlargement of the micelles due to the increase of the molecular weight of PHEMA or PEMA block. In addition, ABG micelles possess higher hydrodynamic diameter compared to DHBG micelles although the chain lengths of PEMA is lower than the PHEMA. The driving force for the micelles formation of amphiphilic surfactant is contact elimination between the hydrophobic core and water molecule through hydrophobic interaction.[43] This interaction is probably accountable for creating bigger micelles interior on the ABGs considering the PHEMA block on DHBGs core is able to interact with water by formation of hydrogen bonds.

CONCLUSIONS

We have successfully synthesized DHBGs of PHEMA-*b*-PGEMA and ABGs of PEMA-*b*-PGEMA in two P(H)EMA compositions by RAFT polymerization method. The structure of both the macro-CTAs and block glycopolymers was well-characterized by ^{1}H NMR spectroscopy. The (H)EMA conversion was maintained below 60% during the macro-CTAs synthesis, resulting in a molecular weight of homopolymers up to 16.6 kg mol^{-1}. In contrast, the GEMA conversion was achieved about 99% in the course of preparation of block glycopolymers with molecular weights in the range of 36.6 to 45.3 kg mol^{-1}. Both P(H)EMA macro-CTAs and block glycopolymers had relatively narrow and monomodal distribution of RI signals as well as moderately low dispersity based on SEC measurements.

The prepared DHBGs and ABGs have displayed to self-assemble into micellar structures in aqueous solutions with the P(H)EMA blocks serving as the core and PGEMA blocks as the corona. Both block glycopolymers had a low CMC of about 0.30 mg mL^{-1} according to fluorescence spectroscopy experiments. Furthermore, the hydrodynamic diameter of the formed micelles was around 9 to 21 nm as obtained from DLS measurements with micelles of DHBGs having lower hydrodynamic diameter than the ABGs.

Considering that the prepared block glycopolymers offer two opposing properties of the micelles core, which can be selected to be either hydrophilic or hydrophobic, it would be interesting to see how this characteristic influence the application of these materials. In addition, the glucosyl part of PGEMA at the micelle corona could possibly be used for interactions with proteins for drug delivery materials, inhibitors of diseases, and biosensors.

ASSOCIATED CONTENT

Supporting Information

The Supporting Information is available free of charge on the ACS Publications website at DOI: 10.1021/acs.biomac.8b01713.

^{1}H NMR spectra of the reaction mixture, SEC measurements of PEMA in THF, and CMC of the ABG micelles (PDF)

AUTHOR INFORMATION

Corresponding Author

*K. Loos. E-mail: k.u.loos@rug.nl. Phone: (31)50-3636867. Fax: (31)50-3636440.

ORCID

Katja Loos: 0000-0002-4613-1159

DOI: 10.1021/acs.biomac.8b01713
Biomacromolecules 2019, 20, 1325−1333

Notes

The authors declare no competing financial interest.

■ ACKNOWLEDGMENTS

The authors kindly appreciate Albert J. J. Woortman for SEC measurements. Indonesia Endowment Fund for Education (Lembaga Pengelola Dana Pendidikan Republik Indonesia/ LPDP RI) scholarship is greatly acknowledged by Azis Adharis for the support of his PhD program.

■ REFERENCES

(1) Becer, C. R.; Hartmann, L. *Glycopolymer Code: Synthesis of Glycopolymers and Their Applications*, 1st ed.; Polymer Chemistry Series; The Royal Society of Chemistry, 2015.
(2) Taylor, M. E.; Drickamer, K. *Introduction to Glycobiology*, 3rd ed.; Oxford University Press: Oxford, 2011.
(3) Miura, Y.; Hoshino, Y.; Seto, H. Glycopolymer Nanobiotechnology. *Chem. Rev.* **2016**, *116* (4), 1673−1692.
(4) Bhatia, S.; Camacho, L. C.; Haag, R. Pathogen Inhibition by Multivalent Ligand Architectures. *J. Am. Chem. Soc.* **2016**, *138* (28), 8654−8666.
(5) Fukuda, T.; Matsumoto, E.; Onogi, S.; Miura, Y. Aggregation of Alzheimer Amyloid Sulfonated Sugar Interface Peptide (1−42) on the Multivalent Sulfonated Sugar Interface. *Bioconjugate Chem.* **2010**, *21* (1), 1079−1086.
(6) Branson, T. R.; Turnbull, W. B. Bacterial Toxin Inhibitors Based on Multivalent Scaffolds. *Chem. Soc. Rev.* **2013**, *42* (11), 4613−4622.
(7) Casas-Solvas, J. M.; Vargas-Berenguel, A. Glycoclusters and Their Applications as Anti-Infective Agents, Vaccines, and Targeted Drug Delivery Systems. In *Carbohydrate Nanotechnology*; Stine, K. J., Ed.; John Wiley & Sons, Inc.: Hoboken, NJ, 2015; pp 175−210.
(8) Utama, R. H.; Jiang, Y.; Zetterlund, P. B.; Stenzel, M. H. Biocompatible Glycopolymer Nanocapsules via Inverse Miniemulsion Periphery RAFT Polymerization for the Delivery of Gemcitabine. *Biomacromolecules* **2015**, *16* (7), 2144−2156.
(9) Appelhans, D.; Klajnert-Maculewicz, B.; Janaszewska, A.; Lazniewska, J.; Voit, B. Dendritic Glycopolymers Based on Dendritic Polyamine Scaffolds: View on Their Synthetic Approaches, Characteristics and Potential for Biomedical Applications. *Chem. Soc. Rev.* **2015**, *44* (12), 3968−3996.
(10) Hushegyi, A.; Klukova, L.; Bertok, T.; Tkac, J. Carbohydrate Nanotechnology and Its Application to Biosensor Development In *Carbohydrate Nanotechnology*; Stine, K. J., Ed.; John Wiley & Sons, Inc.: Hoboken, NJ, 2015; pp 387−421.
(11) Zeng, X.; Qu, K.; Rehman, A. Glycosylated Conductive Polymer: A Multimodal Biointerface for Studying Carbohydrate-Protein Interactions. *Acc. Chem. Res.* **2016**, *49* (9), 1624−1633.
(12) Sunasee, R.; Narain, R. Carbohydrate Nanotechnology Applied to Vaccine Development. In *Carbohydrate Nanotechnology*; Stine, K. J., Ed.; Wiley Online Books; John Wiley & Sons, Inc.: Hoboken, NJ, 2015; pp 369−385.
(13) Lin, K.; Kasko, A. M. Carbohydrate-Based Polymers for Immune Modulation. *ACS Macro Lett.* **2014**, *3* (7), 652−657.
(14) Parry, A. L.; Clemson, N. A.; Ellis, J.; Bernhard, S. S. R.; Davis, B. G.; Cameron, N. R. Multicopy Multivalent" Glycopolymer-Stabilized Gold Nanoparticles as Potential Synthetic Cancer Vaccines. *J. Am. Chem. Soc.* **2013**, *135* (25), 9362−9365.
(15) Adharis, A.; Vesper, D.; Koning, N.; Loos, K. Synthesis of (Meth)Acrylamide-Based Glycomonomers Using Renewable Resources and Their Polymerization in Aqueous Systems. *Green Chem.* **2018**, *20* (2), 476−484.
(16) Becer, C. R. The Glycopolymer Code: Synthesis of Glycopolymers and Multivalent Carbohydrate-Lectin Interactions. *Macromol. Rapid Commun.* **2012**, *33* (9), 742−752.
(17) Pearson, S.; Chen, G.; Stenzel, M. H. Synthesis of Glycopolymers. In *Engineered Carbohydrate-Based Materials for Biomedical Applications*; Narain, R., Ed.; John Wiley & Sons, Inc.: Hoboken, NJ, 2010; pp 1−118.
(18) Loos, K.; Jonas, G.; Stadler, R. Carbohydrate Modified Polysiloxanes, 3: Solution Properties of Carbohydrate-Polysiloxane Conjugates in Toluene. *Macromol. Chem. Phys.* **2001**, *202* (16), 3210−3218.
(19) Loos, K.; Von Braunmühl, V.; Stadler, R.; Landfester, K.; Spiess, H. W. Saccharide Modified Silica Particles by Enzymatic Grafting. *Macromol. Rapid Commun.* **1997**, *18* (10), 927−938.
(20) Muñoz-Bonilla, A.; Fernández-García, M. Glycopolymeric Materials for Advanced Applications. *Materials* **2015**, *8* (5), 2276−2296.
(21) Kiessling, L. L.; Grim, J. C. Glycopolymer Probes of Signal Transduction. *Chem. Soc. Rev.* **2013**, *42* (10), 4476−4491.
(22) Loos, K.; Stadler, R. Synthesis of Amylose-Block-Polystyrene Rod−Coil Block Copolymers. *Macromolecules* **1997**, *30* (24), 7641−7643.
(23) Oh, T.; Nagao, M.; Hoshino, Y.; Miura, Y. Self-Assembly of a Double Hydrophilic Block Glycopolymer and the Investigation of Its Mechanism. *Langmuir* **2018**, *34* (29), 8591−8598.
(24) Park, H.; Walta, S.; Rosencrantz, R. R.; Körner, A.; Schulte, C.; Elling, L.; Richtering, W.; Boker, A. Micelles from Self-Assembled Double-Hydrophilic PHEMA-Glycopolymer-Diblock Copolymers as Multivalent Scaffolds for Lectin Binding. *Polym. Chem.* **2016**, *7*, 878−886.
(25) Quan, J.; Shen, F. W.; Cai, H.; Zhang, Y. N.; Wu, H. Galactose-Functionalized Double-Hydrophilic Block Glycopolymers and Their Thermoresponsive Self-Assembly Dynamics. *Langmuir* **2018**, *34* (36), 10721−10731.
(26) Xu, M. R.; Shi, M.; Bremner, D. H.; Sun, K.; Nie, H. L.; Quan, J.; Zhu, L. M. Facile Fabrication of P(OVNG-Co-NVCL) Thermoresponsive Double-Hydrophilic Glycopolymer Nanofibers for Sustained Drug Release. *Colloids Surf., B* **2015**, *135*, 209−216.
(27) Zhang, Q.; Wilson, P.; Anastasaki, A.; McHale, R.; Haddleton, D. M. Synthesis and Aggregation of Double Hydrophilic Diblock Glycopolymers via Aqueous Set-LRP. *ACS Macro Lett.* **2014**, *3* (5), 491−495.
(28) Pasparakis, G.; Alexander, C. Sweet Talking Double Hydrophilic Block Copolymer Vesicles. *Angew. Chem., Int. Ed.* **2008**, *47* (26), 4847−4850.
(29) Kloosterman, W. M. J.; Roest, S.; Priatna, S. R.; Stavila, E.; Loos, K. Chemo-Enzymatic Synthesis Route to Poly(Glucosyl-Acrylates) Using Glucosidase from Almonds. *Green Chem.* **2014**, *16* (4), 1837−1846.
(30) Han, K. J.; Oh, J. H.; Park, S. J.; Gmehling, J. Excess Molar Volumes and Viscosity Deviations for the Ternary System N,N-Dimethylformamide + N-Methylformamide + Water and the Binary Subsystems at 298.15 K. *J. Chem. Eng. Data* **2005**, *50* (6), 1951−1955.
(31) Ren, R.; Wang, Y.; Sun, W. Design, Synthesis, Characterization and Magnetic Studies of the Metal-Quinolate PHEMA-b-HQ Polymer Micelles. *React. Funct. Polym.* **2016**, *106*, 57−61.
(32) Perrier, S. 50th Anniversary Perspective: RAFT Polymerization - A User Guide. *Macromolecules* **2017**, *50* (19), 7433−7447.
(33) Keddie, D. J. A Guide to the Synthesis of Block Copolymers Using Reversible-Addition Fragmentation Chain Transfer (RAFT) Polymerization. *Chem. Soc. Rev.* **2014**, *43* (2), 496−505.
(34) Moad, G.; Rizzardo, E.; Thang, S. H. Living Radical Polymerization by the RAFT Process − A Third Update. *Aust. J. Chem.* **2012**, *65* (8), 985−1076.
(35) Beers, K. L.; Boo, S.; Gaynor, S. G.; Matyjaszewski, K. Atom Transfer Radical Polymerization of 2-Hydroxyethyl Methacrylate. *Macromolecules* **1999**, *32* (18), 5772−5776.
(36) Weaver, J. V. M.; Bannister, I.; Robinson, K. L.; Bories-Azeau, X.; Armes, S. P.; Smallridge, M.; McKenna, P. Stimulus-Responsive Water-Soluble Polymers Based on 2-Hydroxyethyl Methacrylate. *Macromolecules* **2004**, *37* (7), 2395−2403.
(37) Brosnan, S. M.; Schlaad, H.; Antonietti, M. Aqueous Self-Assembly of Purely Hydrophilic Block Copolymers into Giant Vesicles. *Angew. Chem., Int. Ed.* **2015**, *54* (33), 9715−9718.

DOI: 10.1021/acs.biomac.8b01713
Biomacromolecules 2019, 20, 1325−1333

(38) Willersinn, J.; Bogomolova, A.; Cabré, M. B.; Schmidt, B. V. K. J. Vesicles of Double Hydrophilic Pullulan and Poly(Acrylamide) Block Copolymers: A Combination of Synthetic- and Bio-Derived Blocks. *Polym. Chem.* **2017**, *8* (7), 1244−1254.
(39) Schmidt, B.; Double, V. K. J. Hydrophilic Block Copolymer Self-Assembly in Aqueous Solution. *Macromol. Chem. Phys.* **2018**, *219* (1−5), 1700494.
(40) Aguiar, J.; Carpena, P.; Molina-Bolívar, J. A.; Carnero Ruiz, C. On the Determination of the Critical Micelle Concentration by the Pyrene 1:3 Ratio Method. *J. Colloid Interface Sci.* **2003**, *258* (1), 116−122.
(41) Domínguez, A.; Fernández, A.; González, N.; Iglesias, E.; Montenegro, L. Determination of Critical Micelle Concentration of Some Surfactants by Three Techniques. *J. Chem. Educ.* **1997**, *74* (10), 1227−1231.
(42) Le Zhao, C.; Winnik, M. A.; Riess, G.; Croucher, M. D. Fluorescence Probe Techniques Used To Study Micelle Formation in Water-Soluble Block Copolymers. *Langmuir* **1990**, *6* (2), 514−516.
(43) Holmberg, K.; Jönsson, B.; Kronberg, B.; Lindman, B. Surfactant Micellization. In *Surfactants and Polymers in Aqueous Solution*; John Wiley & Sons, Ltd: West Sussex, 2003; pp 39−66.
(44) Mok, M. M.; Thiagarajan, R.; Flores, M.; Morse, D. C.; Lodge, T. P. Apparent Critical Micelle Concentrations in Block Copolymer/Ionic Liquid Solutions: Remarkably Weak Dependence on Solvophobic Block Molecular Weight. *Macromolecules* **2012**, *45* (11), 4818−4829.
(45) Lee, R.-S.; Wu, K.-P. Synthesis and Characterization of Temperature-Sensitive Block-Graft PNiPAAm-b-(PαN3CL-g-Alkyne) Copolymers by Ring-Opening Polymerization and Click Reaction. *J. Polym. Sci., Part A: Polym. Chem.* **2011**, *49* (14), 3163−3173.
(46) Astafieva, I.; Khougaz, K.; Eisenberg, A. Micellization in Block Polyelectrolyte Solutions. 2. Fluorescence Study of the Critical Micelle Concentration as a Function of Soluble Block Length and Salt Concentration. *Macromolecules* **1995**, *28* (21), 7127−7134.
(47) Iglesias, E. Enolization of Benzoylacetone in Aqueous Surfactant Solutions: A Novel Method for Determining Enolization Constants. *J. Phys. Chem.* **1996**, *100* (30), 12592−12599.
(48) van der Vlist, J.; Faber, M.; Loen, L.; Dijkman, T. J.; Asri, L. A. T. W.; Loos, K. Synthesis of Hyperbranched Glycoconjugates by the Combined Action of Potato Phosphorylase and Glycogen Branching Enzyme from Deinococcus Geothermalis. *Polymers (Basel, Switz.)* **2012**, *4* (1), 674−690.
(49) Le Meins, J. F.; Houg, C.; Borsali, R.; Taton, D.; Gnanou, Y. Morphological Changes Induced by Addition of Polystyrene to Dextran-Polystyrene Block Copolymer Solutions. *Macromol. Symp.* **2009**, *281* (1), 113−118.

DOI: 10.1021/acs.biomac.8b01713
Biomacromolecules 2019, 20, 1325−1333